Pose-Invariant Eye Gaze Estimation Using Geometrical Features of Iris and Pupil Images

Mohammad Reza Mohammadi*
Electrical Engineering, M.Sc. Student, Amirkabir University of Technology
mrmohammado@aut.ac.ir
Abolghasem A. Raie
Electrical Engineering, Associate Professor, Amirkabir University of Technology
raie@aut.ac.ir

Abstract

In the cases of severe paralysis in which the ability to control the body movements of a person is limited to the muscles around the eyes, eye movements or blinks are the only way for the person to communicate. Interfaces that assist in such communications often require special hardware or reliance on active infrared illumination. In this paper, we propose a non-intrusive algorithm for eye gaze estimation that works with video input from an inexpensive camera and without special lighting. The main contribution of this paper is proposing a new geometrical model for eye region that only requires the image of one iris for gaze estimation. Essential parameters for this system are the best fitted ellipse of the iris and the pupil center. The algorithms used for both iris ellipse fitting and pupil center localization pose no pre-assumptions on the head pose. All in all, the achievement of this paper is the robustness of the proposed system to the head pose variations. The performance of the method has been evaluated on both synthetic and real images leading to errors of 2.12 and 3.48 degrees, respectively.

Keywords: Gaze Estimation, Projective Geometry, Video-Based Human–Computer Interface, Pupil Center Localization, Iris Ellipse Fitting.

1. Introduction

Eye gaze estimation is utilized in many applications such as driver alertness systems [1,2], psychological researches and determining comprehension while reading texts or watching TV programs [3-5], handicapped rehabilitation and human–computer interaction (HCI) [6,7] which has received attention in the research community in more recent years.

All proposed algorithms of gaze estimation may be classified in two groups. Algorithms in the first group require special devices such as electrodes, special glasses or hats [8-10]. In contrast, algorithms in the second group use one (or much) non-contact camera and computer vision techniques to estimate the gaze direction [7, 11-18]. In most cases, algorithms of the first group result in higher accuracy, but for two reasons they cannot become universal. The first reason is their high cost due to using especial devices. The second one is the contact of their devices to the user body. So, the user cannot be comfortable when using them. Because of this contact, the first group is called "intrusive" and the second one "non-intrusive". Fig. 1 shows two examples of intrusive and non-intrusive systems.

Fig. 1: Two samples of systems used in intrusive (top row) and non-intrusive (bottom row) methods [7, 17].

Many of the current camera-based interfaces that estimate eye gaze direction make use of active infrared illumination [11-14]. In many approaches, the infrared light reflects off the back of the eye to create a distinct "bright pupil effect" in the image. The light is synchronized with the camera to illuminate the eyes in alternate frames. The eyes are then located by comparing a frame with this bright pupil effect with a subsequent frame without the illuminated

* Corresponding Author

pupils. Typically, the relative gaze direction of an eye is found by analyzing the difference between the center of the bright eye pixel area and the reflection off the surface of the eye from the light source. There is a concern that infrared camera-based interfaces require a complicated calibration procedure which is difficult for small children to follow [7]. However, conventional (non-infrared) cameras are more available and the algorithms that work with them are more applicable.

In recent years, some systems have been proposed that do not require special lighting [7, 15-19]. These systems can be very practical. The principles of such systems are similar. First, the face of the user detects and then determines the location of his/her eyes. The last and the most important step of these algorithms is the estimation of the gaze direction from the eyes and other face landmarks.

Authors in [7] used symmetry between two eyes to classify gaze direction to 3 sides (center, left and right). In the proposed algorithm of [15], a circle is fitted to the iris boundary using Hough transform. Then, current gaze direction is determined by calculating the distance of the iris center from the iris position when it is looking forward. In this algorithm, the gaze direction is divided to 9 directions. In [16] coordinates of the center of mass of the eye region is computed and used to train an MLP (Multilayer Perceptron) to classify any gaze in 4 directions.

In the above algorithms, direction of gaze is limited to some sides. In other algorithms such as [17] gaze direction is represented as a vector in 3D space. In [17], a camera is used to detect the face location and then a pan/tilt/zoom camera with high resolution is used to zoom on the right eye. Finally, the authors in [17] have used geometry of eye in 3D and its projection to 2D to obtain the gaze vector. Using 2 cameras with high resolution and zooming ability for them are the most drawbacks of that algorithm.

In [7, 15, 16], rotation and displacement of the head are limited severely. This problem (limited rotation and displacement for the head) is popular in most of the gaze estimation systems and is very important in a practical system. In [17], another accurate system is used to estimate the eye corners positions in 3D. By adding this system, the authors in [17] claim that their final system is robust to head rotation. Therefore, their system is very expensive. Because of this, we propose an algorithm for gaze estimation that is robust to rotation and displacement of head and does not require another system. The proposed system requires only an inexpensive camera; so,

it can be practical for usage. An algorithm box of the approach is given in Fig. 2.

The first step in this algorithm is face and eyes detection and the Viola-Jones algorithm [20] is used to implement them. The focus of this paper is on the next steps. In this paper, a new geometrical model for eye region is proposed that only requires an image of one iris for gaze estimation. Parameters required for gaze estimation in this model are the iris ellipse and the pupil center that novel algorithms are used to compute them.
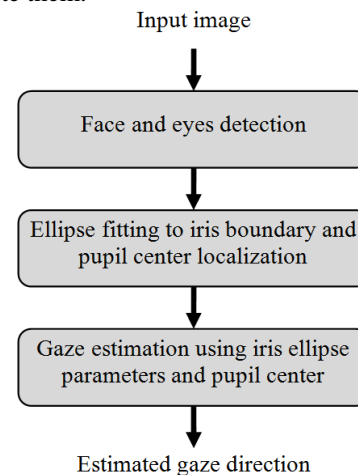

Fig. 2: Block diagram of the proposed gaze estimation approach.

The remainder of this paper is structured as follows. The proposed geometrical model for eye region and the approach to estimate the eye gaze from the iris image are discussed in Section 2 and Section 3, respectively. Experimental results are given on simulated data as well as on real images in section 4. The paper is concluded in Section 5.

2. Eye Model

Fig. 3 shows a physiological model of eye [21]. From this figure, it can be found that the eyeball is like a sphere and the iris boundary is a circle located on the surface of the eyeball. Also, the pupil is a hole on the iris surface with a circle boundary and its center coincides with the iris center. The gaze direction is approximated using a vector that passes through the eyeball center and the iris center [17].

The cornea is the transparent front part of the eye with refractive index of 1.376 that covers the iris, pupil, and anterior chamber [21] and may be regarded as a single spherical surface [22]. The anterior chamber is filled with transparent aqueous humour with refractive index of 1.336 [21], which is close to the refractive index of

cornea. This combination of cornea and aqueous humour acts similar to a plano-convex lens on the surface of the iris. From the camera stand point, considering the position of iris boundary and this plano-convex lens in Fig. 3, the image of the iris border is not affected, but the image of iris surface, including the pupil boundary is affected by refractive property of the lens. The image of pupil boundary from behind of the plano-convex lens, while being in focal distance, appears to the camera a bit larger circle and farther away with the center on the gaze vector [23]. Thus, in image space, the two boundaries of iris and pupil are no longer co-centered.
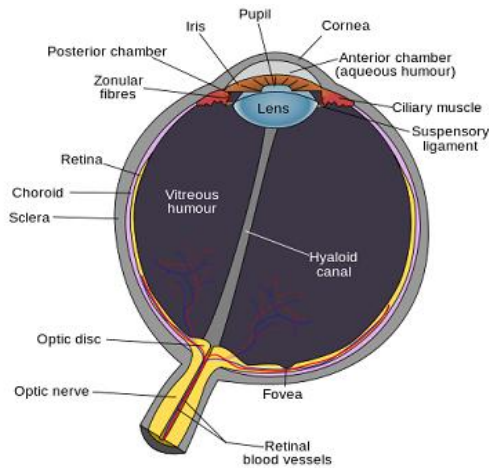

Fig. 3: A biological model of eye [21].

Hence, Fig. 4 is proposed as a simplified eye geometrical model in image space. In this model, the eyeball is a sphere with radius R. The iris boundary is a circle located on the eyeball surface and the distance between the eyeball center and the iris center is denoted by d_i. The pupil boundary is also a circle and the distance between the eyeball center and the pupil center is d_p while $d_p < d_i$. In addition, the gaze direction in the image space is a vector that passes from the eyeball center, the pupil center and the iris center. The eye geometrical model in [17] is similar to Fig. 4; however, the pupil position being a key element in unique solution selection procedure is not defined in it. This concept is discussed later.
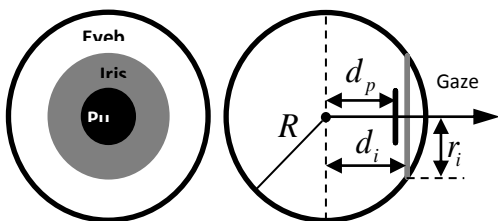

Fig. 4: Proposed geometrical model for eye region and gaze direction.

When changing the eye gaze, the eyeball rotates around its center and the 2D image of eye region may change. Fig. 5 shows three examples of different gaze directions. As can be observed in Fig. 5 and can be proved with projective geometry, the boundary of the iris and the pupil convert to ellipses. So, if an ellipse can fit to the iris boundary, gaze direction may be computed by its parameters. However, for gaze directions that are symmetric about the perpendicular vector to the camera plane (like the first and the third parts in Fig. 5), the iris ellipses are identical. In other words, the iris ellipse parameters return two solutions for gaze direction, but, only one of them is valid. As can be seen in Fig. 5, the position of the pupil in the iris region can separate two symmetric cases. Consideration of this feature for unique solution selection is the main contribution of this model.

Fig. 5: Three different gaze directions and their effects on the 2D images of the iris boundary and the pupil position.

3. Approach of Gaze Estimation

3.1 Gaze direction formulas using the iris boundary

As presented in previous part, it is assumed that the iris contour is a circle and the gaze vector is the normal vector to this circle passing through the eyeball center. From projective geometry, it is proved that the shape of the rotated circle when projected to 2D is an ellipse. But, when we have an ellipse, it can be created from 2 different circles in 3D. Fig. 6 shows an example of this issue. Part (a) of this figure is an ellipse in 2D space and part (b) shows 2 circles in 3D that can be converted to that ellipse by projection. In this figure, darker colors are related to closer sides of circle to the camera. So, if an ellipse can fit to the iris boundary, the gaze vector may be computed from its parameters (two solutions). In this part, the equations of these two ellipses are derived and in the next part, a novel method to select the true solution is proposed.
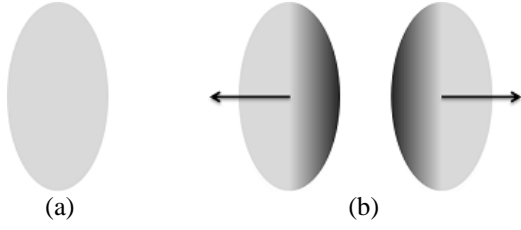
Fig. 6: An ellipse in 2D can be created from projection of two different circles in 3D, (a) an ellipse in 2D, and (b) two corresponding circles in 3D.

Fig. 7 shows an ellipse in 2D space. Parametric equations of such ellipse are as (1) and (2):

$$x(t) = h + a\cos(t)\cos(\varphi) - b\sin(t)\sin(\varphi), \quad (1)$$

$$y(t) = k + a\cos(t)\sin(\varphi) + b\sin(t)\cos(\varphi), \quad (2)$$

where t is a parameter that changes from 0 to 360 degrees; a and b are the major and minor radii, respectively; h and k are the ellipse center coordinate in x and y directions, respectively; φ is the angle between major radius of the ellipse and x direction.
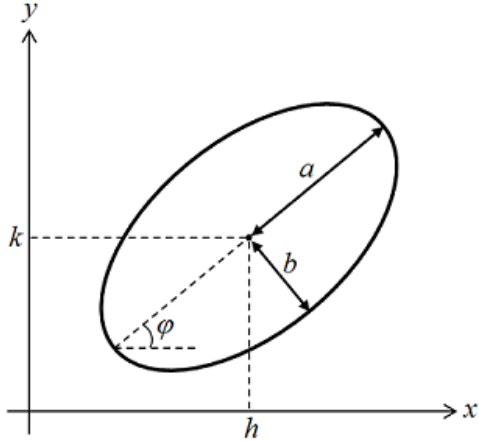

Fig. 7: An ellipse in 2D space.

If a circle with radius r_i rotates about z-axis by θ and about x-axis by ϕ (Fig. 8), equations (3) to (7) are its ellipse parameters:

$$a_i = r_i, \quad (3)$$

$$b_i = r_i \cos(\theta), \quad (4)$$

$$h_i = d_i \sin(\theta)\cos(\phi), \quad (5)$$

$$k_i = d_i \sin(\theta)\sin(\phi), \quad (6)$$

$$\varphi_i = \phi + \pi/2 + k\pi, \quad k = 0,1, \quad (7)$$

where in (5) and (6) d_i is the distance between the eyeball and the iris centers and can be computed from (8):

$$d_i = \sqrt{R^2 - r_i^2}. \quad (8)$$

Now, it is required to compute the invert equations to obtain gaze parameters (θ and ϕ)

from ellipse parameters. Using (3), (4) and (7), (9) to (11) can be derived:

$$r_i = a_i, \quad (9)$$

$$\theta = \cos^{-1}(b_i/a_i), \quad (10)$$

$$\phi = \varphi_i - \pi/2 - k\pi, \quad k = 0,1. \quad (11)$$

Also, if (5) and (6) are used, (12) may be obtained as another solution for ϕ:

$$\phi = \text{atan2}(k_i, h_i), \quad (12)$$

where atan2 is the arctangent function with two arguments. However, values of k_i and h_i should be related to the eyeball center and this parameter is unknown. So, we cannot use (12) directly.
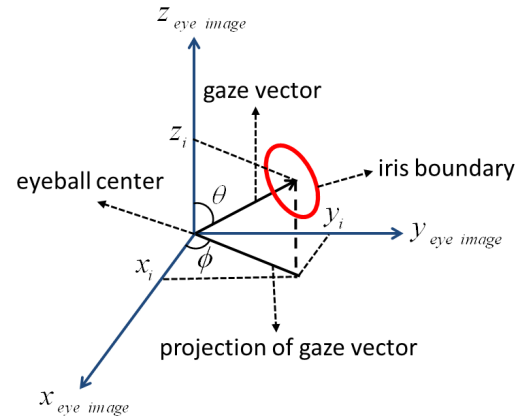

Fig. 8: Coordinate system of the proposed approach.

3.2 Unique solution selection using the pupil center

In [17], it is assumed that eye corners are located on the eyeball sphere. In addition, in [17], it is assumed that he ratio of the eyeball radius to the iris radius is a generic constant. So, their technique is as follows:

1. The eyeball radius estimated by multiplying the iris radius and the generic constant.
2. Two eyeball centers computed with respect to gaze directions and the eyeball radius.
3. Distances of two eyeball centers from two eye corners computed.
4. True solution is one that distances of two eye corners from the related eyeball center are approximately equal.

The main problem in this technique is the requirement to eye corners coordinates in 3D. Accurately localization of eye corners in 3D images is a very hard problem which requires another expensive system. To avoid this requirement, a novel technique obtained from the eye model and projective geometry is proposed. This technique is further discussed.

In previous part, Fig. 4 was proposed for eye model. From this figure, if eye rotates about the eyeball center, new coordinates of the pupil center in 2D image can be obtained from (13) and (14):

$$h_p = d_p \sin(\theta)\cos(\phi), \tag{13}$$

$$k_p = d_p \sin(\theta)\sin(\phi). \tag{14}$$

In (13) and (14) d_p is the distance between the eyeball and the pupil centers. From these equations, the gaze parameter ϕ may be computed as in (15):

$$\phi = \operatorname{atan2}(k_p, h_p). \tag{15}$$

Because the eyeball center coordinate is unknown, we cannot use (15) directly, like (12). To use (12) and (15), a relative equation between the iris and the pupil centers by ϕ is obtained. In previous part, it is shown that in the image space the pupil center is observed to be closer to the eyeball center than the iris center. On the other hand, from (12) and (15) it can be found that coordinate of the pupil and the iris centers are on a line with angle ϕ. Fig. 9 shows this issue that the iris and the pupil centers are located on a line with angle ϕ as well as the reality that the pupil center is closer to the eyeball center. So, if a line connects the pupil center to the iris center, the direction of that line may be equal to ϕ. Therefore, (16) is obtained for ϕ without requiring to know the eyeball center coordinates:

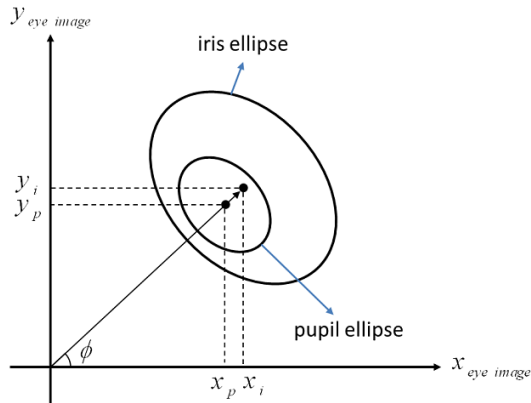$$\phi = \operatorname{atan2}(k_i - k_p, h_i - h_p). \tag{16}$$

Fig. 9: Positions of the pupil and the iris centers to the eyeball center.

The centers of the pupil and the iris are close together in a conventional image. Thus, the result of (16) may be less accurate than the true result of (11). Thus, it is proposed to use (16) to select the true solution of (11). In other words, one solution of (11) is selected as the true solution that is closer to the result of (16). Fig. 10 shows the proposed technique for unique solution

selection. Moreover, Fig. 11 shows two real images of eye region with the connecting vectors from the pupil centers to the iris centers. It can be seen from these images that our assumption about the pupil and the iris relation is valid.
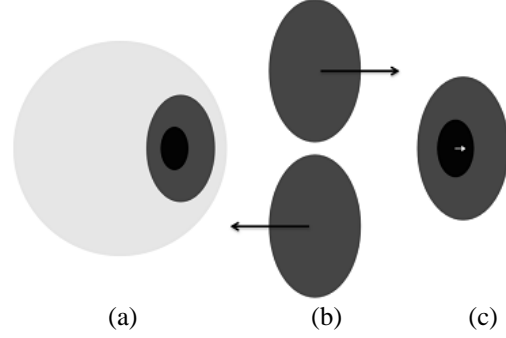
Fig. 10: Unique solution selection based on the position of the pupil center, (a) original image of the eye region, (b) two computed gaze directions with respect to the iris ellipse, and (c) connecting a vector from the pupil center to the iris center and selecting one solution from part (b) which is closer to this vector.
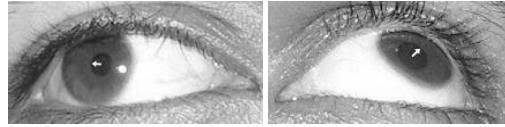
Fig. 11: Connecting the pupil centers to the iris centers for two real images of the eye region.

Table 1 shows the pseudo code of the gaze estimation approach proposed in this paper. In this pseudo code, ϕ_1 is the result of (11) with $k = 0$ and ϕ_2 is the result of (16). In the 6th command, the closeness of ϕ_2 to the solutions of (11) is investigated. If the absolute distance of ϕ_2 from ϕ_1 is lower than 90°, k must be 0 and ϕ_1 is the true solution. Otherwise, the absolute distance of ϕ_2 from ϕ_1-π will be lower than 90° and k should be 1.

Table 1: Pseudo code of the proposed approach for gaze estimation

Input: an image of one iris
1) Iris ellipse fitting
2) Pupil center localization
3) Compute θ using iris ellipse radii: $$\theta = \cos^{-1}(b_i / a_i)$$
4) Compute ϕ_1 using iris ellipse angle: $$\phi_1 = \varphi_i - \pi/2$$
5) Compute ϕ_2 using iris end pupil centers: $$\phi_2 = \operatorname{atan2}(k_i - k_p, h_i - h_p)$$
6) If $\cos(\phi_2 - \phi_1) > 0$: $$\phi = \phi_1$$ Otherwise $$\phi = \phi_1 - \pi$$
Output: θ and ϕ

3.3 Sensitivity of the proposed model to the requiring parameters

In this part, the sensitivity of rotation angles in the proposed model w.r.t. requiring parameters is calculated. Angle θ has dependency only upon the ratio of the iris and pupil ellipse radii. So, its sensitivity can be calculated as (17):

$$\frac{d\theta}{d(b/a)} = \frac{-1}{\sqrt{1-(b/a)^2}}.$$

$$(17)$$

Equation (17) expresses that maximum sensitivity of the proposed algorithm is when two radii of ellipse are equal and its minimum is when the minor radius is zero. In other words, when user looks straight to the camera, the sensitivity of the algorithm is max.

Angle ϕ in (11) has a direct relationship to φ; so its sensitivity to φ is 1. On the other hand, for unique solution selection ϕ depends on the pupil center coordinates. Dependency of ϕ upon the pupil center coordinates is discrete since it specifies that k is 0 or 1 in (11). Thus, sensitivity of ϕ to the pupil center coordinates is infinite.

Because of the high sensitivity of θ to diameters of the iris ellipse and ϕ to the pupil center coordinates, algorithms which compute these parameters with high accuracy are required. So, two recently accurate algorithms for iris ellipse fitting [24] and pupil center localization [25] by the authors are used.

4. Experimental Results

The proposed algorithms will be tested first with synthetic and then with real images.

4.1 Experimental results on synthetic images

In this section, to evaluate the performance of the proposed algorithm, we create some sets of synthetic images and apply the algorithm on them.

4.1.1 Synthetic images creation

The proposed geometrical model of eye is used to create the synthetic images. Four samples of these images with the fitted iris ellipse and the estimated gaze direction are shown in Fig. 12. In these images, it is assumed that the eyeball center is located at the origin of the coordinate system. The eyeball, the iris and the pupil radii and ratio of d_p to d_i are assumed to be 1.5, 0.6, 0.15 and 0.9, respectively. Also, it is assumed that eye corners are at (-1.4 , 0) and (1.4 , 0). Upper and lower eyelids pass from (0 , 0.6) and (0 , -0.4), respectively. These assumptions are

based on anatomical features of the eye region for human beings.

The algorithm was tested on some sets of synthetic images with different sizes (150×100, 300×200 and 600×400) and the effect of eyelid occlusion was checked.
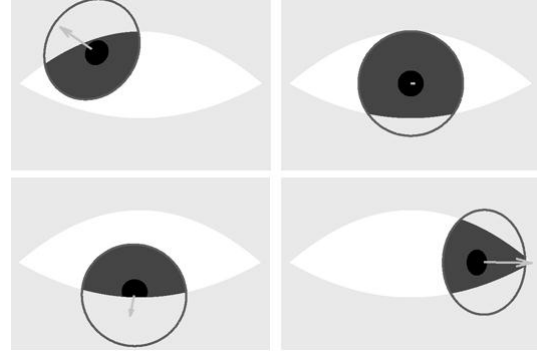

Fig. 12: Fitted ellipse to the iris boundary and estimated gaze direction for 4 samples of the synthetic images.

4.1.2 Accuracy of the proposed algorithm

To evaluate the performance of the proposed algorithm, 5111 images are created for $0 \le \theta \le 35$ and $0 \le \phi \le 360$. However, only 3739 of them, in which less than half of their pupils are occluded by eyelids, are used. The average errors of the proposed algorithm in different sizes (with and without considering eyelid occlusion) are listed in Table 2. As can be seen, the average error of the proposed algorithm is increased when the size of the images decreases. Moreover, by considering eyelid occlusion, pixels on the iris boundary reduced, so, the error of the ellipse fitting algorithm and thereby, the error of the proposed gaze estimation approach increase.

Table 2: The average error of the proposed algorithm on the synthetic images by different sizes (in degrees)

Size of images	150×100	300×200	600×400
With eyelid occlusion	2.1160	0.8462	0.3855
Without eyelid occlusion	0.5880	0.2163	0.0825

It is notable that for the synthetic images by the proposed model, any error for the unique solution selection cannot be occurred. In other words, all of the reported errors in Table 2 are related to the error of the ellipse fitting algorithm. The ellipse fitting algorithm is not under scope of this paper; however, analyzing of the errors can be very interesting.

To analyze the error of the proposed algorithm in more details, the average error for different values of θ (changing ϕ) is plotted in Fig. 13. As can be observed, the maximum error

of the proposed algorithm occurs in $\theta = 0$, whose reason is the high sensitivity of the proposed model for this case. As θ increased, sensitivity of the model reduced, but, more pixels of the iris boundary covered by eyelids and error of the fitted ellipse increased. So, the overall behavior of the average error is descending versus θ, but, in some points, the average error shows a small increasing behavior.
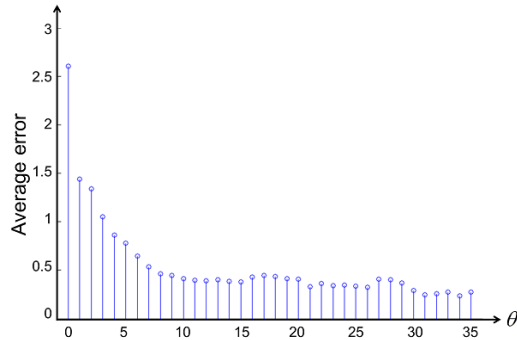

Fig. 13: The average error of the proposed algorithm for different values of θ (changing ϕ).

The average error for different values of ϕ (changing θ) is shown in Fig. 14. We find some important notes in this figure:

1. The average error has two maximum values at angles about 90 and 270 degrees. In these angles, only one part of the iris boundary is observable and the error of their ellipse fitting is high.
2. Values of the maxima are different. Existing difference on concavity for upper and lower eyelids is the reason of this phenomenon.
3. The average error has two minimum values at angles about 0 and 180 degrees. In these angles, two different parts of the iris boundary are observable and the error of their ellipse fitting is low.
4. Locations of the minimum values are not exactly on the 0 and 180 degrees. They have leanings toward the 90 degrees (about 10 and 170 degrees). Its reason is that the concavity of the upper eyelid is higher than the lower one.

Thus, it can be concluded that horizontal error of the proposed algorithm is lower than the vertical one. In addition, eyelid occlusion affects the average error directly.

4.2 Experimental results on real images

One of the problems to evaluate the performance of the proposed algorithm is the lack of a proper database. So, we first prepare a database and then apply our algorithms on it.
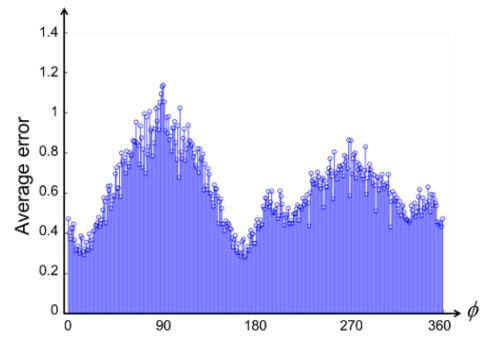

Fig. 14: The average error of the proposed algorithm for different values of ϕ (changing θ).

4.2.1 Database preparation

To evaluate the performance of a gaze estimation algorithm, some images whose gaze directions were known are needed. So, a device that its model can be observed in Fig. 15 is made. In this device a board with sizes of 50cm×50cm and 30 points plotted on it is used. With 40cm distance from the board, there is a location for user's chin that fixes the distance of the user eyes by the floor of the device to approximately 25cm.
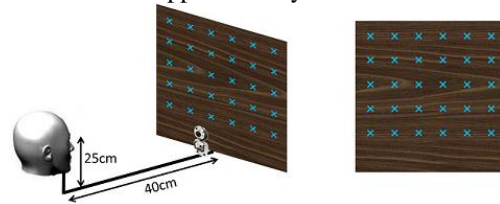

Fig. 15: Two views of the designed device to prepare the gaze estimation database.

The implemented device is shown in Fig. 16. Camera is located at the bottom of the device. This location has two main reasons. First, in real applications, camera cannot be located on the center of the plane which is usually a monitor. So, camera should be located at the top or the bottom of the plane. Second, when the user looks at the bottom of the plane, his upper eyelid covers much of his iris region. In this case, if the image is captured from the bottom of the plane, the iris region is larger in the image. Therefore, the accuracy of the system may be higher than that of a camera located at the top of the plane.
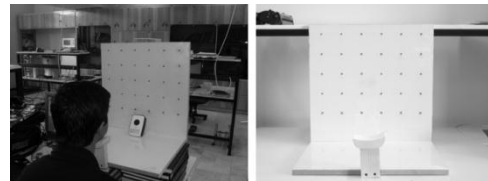

Fig. 16: Two views of the made device to prepare the gaze estimation database.

We got the images from 10 persons. So, the created database has 300 images one of them is shown in Fig. 17.

Fig. 17: A sample image of the created database.

4.2.2 Accuracy of the proposed algorithm

Four samples of the estimated gaze direction, for the images on the database, are shown in Fig. 18. In this figure, the fitted ellipse for two eyes and the estimated gaze direction for them are shown.

Table 2: The average error of the proposed algorithm in estimation of the gaze direction for 10 subjects

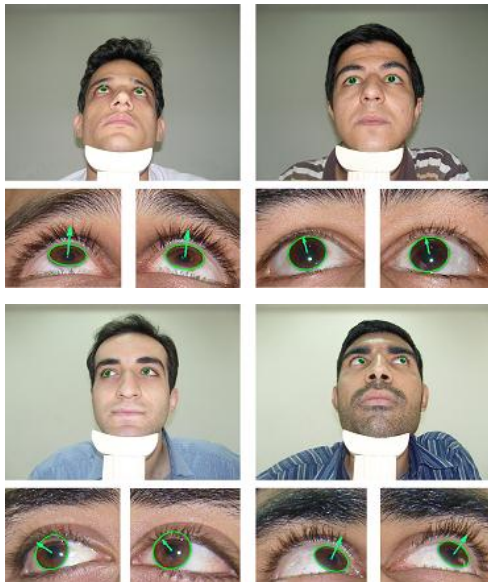| Subject	Error (degrees)
1	4.3512
2	3.6551
3	3.1206
4	3.9568
5	3.6545
6	2.9061
7	2.6699
8	4.6781
9	1.7701
10	4.0473
Average	3.4810

Fig. 18: Four samples of the images in the prepared database and their estimated gaze directions.

The average errors of the proposed algorithm for subjects in the database are listed in Table 3. For the 300 images in the database, the average error 3.48 degrees is obtained.

4.3 Sensitivity of the proposed model to head rotation

An important property of the proposed algorithm is its robustness to head rotation. In the proposed model for gaze estimation, only geometrical properties of the iris and the pupil are used. So, if we fit a proper ellipse to the iris boundary and localize the pupil center, the direction of gaze may be estimated without requiring the information of head rotation. Proposed algorithms for iris ellipse fitting [24] and pupil center localization [25] does not use any pre-assumption for head pose; therefore, the proposed system may be robust to head rotation.

There are two different types of the head rotation which are rotation-in-plane (RIP) and rotation-off-plane (ROP) [26] (Fig. 19). RIP is considered to be a rotation about Yaw and Pitch axes and ROP about Roll axis. Fig. 20 shows four images which support all possible head rotations. The eye regions for these images are cropped manually. As can be observed, a proper ellipse is fitted to the iris boundary, and the gaze direction is properly estimated. Therefore, it may be found that the proposed algorithm is robust to head rotations.
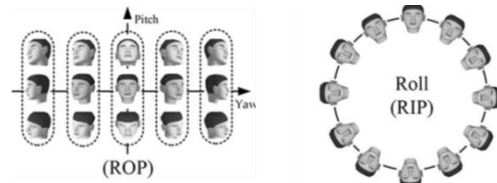

Fig. 19: Different possible head rotations [25].

Fig. 20: Four real images which support different head rotations and estimated gaze directions for them.

4.4 Comparing the proposed system with previous works

Generally speaking, with respect to the experimental results, the average error of the proposed algorithm is about 3.48 degrees. A comparison of the results of this paper with the previous works is listed in Table 4. As can be seen in this table, the average error of the proposed algorithm is lower than the algorithms of [27, 28], but it is higher than algorithms of [17, 29-33]. The main reason for higher accuracy of the algorithms of [17, 29-32] is their equipment. In [29-33], some IR cameras with high zooming capabilities are used which have increased the cost of the system. In addition, algorithm of [17] has employed pan/tilt/zoom cameras as well as a pose estimation system. In contrast, our proposed algorithm and the algorithm of [27] use only an inexpensive webcam. Therefore, the cost of these systems is very lower than the systems of [17, 29-33].

5. Conclusion

In this paper, a non-intrusive method working with video input from an inexpensive camera and without special lighting is presented. As the structures based on desktop cameras are preferred over the head mounted ones according to their ease of use, we used the same structure in our setup. The main contribution of this paper was proposing a new geometrical model for eye region and gaze direction.

To evaluate the performance of the proposed algorithm, we made two sets of synthetic and real images. For real images, the average error of estimated gaze direction was 3.48 degrees.

The sensitivity of the system increases in directions that the subject looks directly toward the camera. To reduce this sensitivity, we can add another camera to the proposed system. In this case, there is always at least one camera which is not in the path of gaze and has low sensitivity. In addition, a hierarchical keyboard can be designed to prepare this system for eye typing.

Table3: Comparing the proposed system by the previous ones

system	Requiring devices	Price	User mode	Horizontal accuracy (degrees)	Vertical accuracy (degrees)
Commercial systems in [28-32]	IR cameras with high zooming ability	Averagely, tens of thousands dollar	Desktop - Head mounted	0.5-1	0.5-1
Proposed system in [17]	Precise pose detection system and two cameras with pan/tilt/zoom ability	-	Desktop	1	1
Proposed system in [26]	IR camera with high zooming ability	-	Desktop	5	8
Proposed system in [27]	Webcam	A few hundred dollars	Desktop	8	8.5
Proposed system in this paper	webcam	A few hundred dollars	Desktop	2.23	3.03

References

[1] P. Smith, M. Shah, and N. da Vitoria Lobo, "Monitoring head/eye motion for driver alertness with one camera," 15th International Conference on Pattern Recognition, pp. 636-642, vol.4, 2000.

[2] B. Bhowmick, and K. S. Chidanand Kumar, "Detection and classification of eye state in IR camera for driver drowsiness identification," IEEE International Conference on Signal and Image Processing Applications, pp. 340-345, 2009.

[3] N. Franck, E. Daprati, F. Michel, M. Saoud, J. Daléry, M. Marie-Cardine, and N. Georgieff, "Gaze discrimination is unimpaired in schizophrenia," Psychiatry Research, vol. 81, no. 1, pp. 67-75, 1998.

[4] D. D. Salvucci, "Inferring intent in eye-based interfaces: tracing eye movements with process models," SIGCHI conference on Human factors in computing systems, Pittsburgh, Pennsylvania, United States, 1999.

[5] Y. Sawahata, R. Khosla, K. Komine, N. Hiruma, T. Itou, S. Watanabe, Y. Suzuki, Y. Hara, and N. Issiki, "Determining comprehension and quality of TV programs using eye-gaze tracking," Pattern Recognition, vol. 41, no. 5, pp. 1610-1626, 2008.

[6] O. Spakov, and P. i. Majaranta, "Scrollable Keyboards for Casual Eye Typing," Psychology Journal, vol. 7, no. 2, pp. 159-173, 2009.

[7] J. J. Magee, M. Betke, J. Gips, M. R. Scott, and B. N. Waber, "A Human-Computer Interface Using Symmetry Between Eyes to Detect Gaze Direction," IEEE Transactions on Systems, Man and Cybernetics, Part A: Systems and Humans, vol. 38, no. 6, pp. 1248-1261, 2008.

[8] D. G. Evans, R. Drew, and P. Blenkhorn, "Controlling mouse pointer position using an infrared head-operated joystick," IEEE Transactions on Rehabilitation Engineering, vol. 8, no. 1, pp. 107-117, 2000.

[9] R. Vaidyanathan, C. Beomsu, L. Gupta, K. Hyunseok, S. Kota, and J. D. West, "Tongue-Movement Communication and Control Concept for Hands-Free Human-Machine Interfaces," IEEE Transactions on Systems, Man and Cybernetics, Part A: Systems and Humans, vol. 37, no. 4, pp. 533-546, 2007.

[10] R. Barea, L. Boquete, M. Mazo, and E. Lopez, "System for assisted mobility using eye movements based on electrooculography," IEEE Transactions on Neural Systems and Rehabilitation Engineering, vol. 10, no. 4, pp. 209-218, 2002.

[11] C. H. Morimoto, D. Koons, A. Amir, and M. Flickner, "Pupil detection and tracking using multiple light sources," Image and Vision Computing, vol. 18, no. 4, pp. 331-335, 2000.

[12] Z. Zhu, and Q. Ji, "Eye and gaze tracking for interactive graphic display," Machine Vision and Applications, vol. 15, no. 3, pp. 139-148, 2004.

[13] P. Kang Ryoung, "A Real-Time Gaze Position Estimation Method Based on a 3-D Eye Model," IEEE Transactions on Systems, Man, and Cybernetics, Part B: Cybernetics, vol. 37, no. 1, pp. 199-212, 2007.

[14] Y. Dong Hyun, and C. Myung Jin, "Non-intrusive eye gaze estimation without knowledge of eye pose," Sixth IEEE International Conference on Automatic Face and Gesture Recognition, pp. 785-790, 2004.

[15] D. B. B. Liang, and H. Lim Kok, "Non-intrusive eye gaze direction tracking using color segmentation and Hough Transform," International Symposium on Communications and Information Technologies, pp. 602-607, 2007.

[16] H. M. Peixoto, A. M. G. Guerreiro, and A. D. D. Neto, "Image processing for eye detection and classification of the gaze direction," International Joint Conference on Neural Networks, pp. 2475-2480, 2009.

[17] J. G. Wang, E. Sung, and R. Venkateswarlu, "Estimating the eye gaze from one eye," Computer Vision and Image Understanding, vol. 98, pp. 83-103, 2005.

[18] M. R. Mohammadi, and A. Raie, "Robust pose-invariant eye gaze estimation using geometrical features of iris and pupil image," 20th Iranian Conference on Electrical Engineering, pp. 593-598, 2012.

[19] M. R. Mohammadi, and A. Raie, "Selection of Unique Gaze Direction Based on Pupil Position," IET Computer Vision, vol. 7, 2013.

[20] P. A. Viola, and M. J. Jones, "Robust Real-Time Face Detection," International Journal of Computer Vision, vol. 57, no. 2, pp. 137-154, 2004.

[21] http://en.wikipedia.org/wiki/Eye.

[22] A. Villanueva, and R. Cabeza, "Evaluation of Corneal Refraction in a Model of a Gaze Tracking System," IEEE Transactions on Biomedical Engineering, 2008, vol. 55, no. 12, pp. 2812-2822.

[23] http://en.wikipedia.org/wiki/Lens_(optics)

[24] M. R. Mohammadi, and A. Raie, "A Novel Accurate Algorithm to Ellipse Fitting for Iris Boundary Using Most Iris Edges," Journal of American Science, vol. 8, 2012.

[25] M. R. Mohammadi and A. Raie, "A Novel Technique for Pupil Center Localization Based on Projective Geometry," 7th Iranian Conference on Machine Vision and Image Processing, pp. 1-5, 2011.

[26] H. Chang, A. Haizhou, L. Yuan, and L. Shihong, "High-Performance Rotation Invariant Multiview Face Detection," IEEE Transactions on Pattern Analysis and Machine Intelligence, vol. 29, no. 4, pp. 671-686, 2007.

[27] Z. Zhu, K. Fujimura, and Q. Ji, "Real-time eye detection and tracking under various light conditions," Symposium on Eye tracking research & applications, New Orleans, Louisiana, 2002.

[28] P. Majaranta and K.-J. Räihä, "Text entry by gaze: Utilizing eye-tracking," Text entry systems: Mobility, accessibility, universality, pp. 175-187, 2007.

[29] http://www.eyecan.ca, 2012.

[30] http://www.eyegaze.com, 2012.

[31] http://www.eyetechds.com, 2012.

[32] http://www.sr-research.com, 2012.

[33] http://www.tobii.com, 2012.

Mohammad Reza Mohammadi was born in Qom in Iran, on July 25, 1987. He received BSc and MSc degrees both in electrical engineering with rank one from Amirkabir University of Technology (Tehran Polytechnic). He is currently PhD candidate of electrical engineering in Sharif University of Technology. His interests and researches include Machine Vision and Machine Learning.

Abolghasem Asadollah Raie received the B.Sc. degree in Electrical Engineering from Sharif University of Technology, Iran, in 1973 and the M.Sc. and Ph.D. degrees in Electrical Engineering from University of Minnesota, USA, in 1979 and 1982, respectively. Currently, he is an Associate Professor with the Electrical Engineering Department of AmirKabir University of Technology, Iran. His research interests are algorithm design and performance analysis, machine vision, sensor fusion, and mobile robots navigation.